Predicting Harmful Algal Blooms Using Ensemble Machine Learning Models and Explainable AI Technique: A Comparative Study

Omer Mermer[1], Eddie Zhang[1,2], Ibrahim Demir[1,2,3]

[1] IIHR—Hydroscience and Engineering, University of Iowa, Iowa City, Iowa, USA
[2] The Harker School, San Jose, California, USA
[3] Civil and Environmental Engineering, University of Iowa, Iowa City, Iowa, USA
[4] Electrical and Computer Engineering, University of Iowa, Iowa City, Iowa, USA

* Corresponding Author, Email: Omer Mermer, omer-mermer@uiowa.edu

Abstract

Harmful Algal Blooms (HABs), driven by environmental pollution, pose significant threats to water quality, public health, and aquatic ecosystems. This study aims to enhance the prediction of HABs in Lake Erie, part of the Great Lakes system, by utilizing ensemble machine learning (ML) models coupled with explainable artificial intelligence (XAI) for interpretability. Using water quality data from 2013 to 2020, various physical, chemical, and biological parameters were analyzed to predict chlorophyll-a (Chl-a) concentrations, a proxy for algal blooms. The study employed multiple ensemble ML models, including Random Forest (RF), Deep Forest (DF), Gradient Boosting (GB), and XGBoost, and compared their performance against individual models such as Support Vector Machine (SVM), Decision Tree (DT), and Multi-Layer Perceptron (MLP). The findings reveal that ensemble models, particularly XGBoost and Deep Forest (DF), achieve superior predictive accuracy with R^2 values of 0.8517 and 0.8544, respectively. The application of SHapley Additive exPlanations (SHAP) provided insights into the relative importance of input features, identifying Particulate Organic Nitrogen (PON), Particulate Organic Carbon (POC), and Total Phosphorus (TP) as critical factors influencing Chl-a concentrations. This research demonstrates the effectiveness of integrating ensemble ML models with XAI to improve HAB prediction accuracy and interpretability. The results support the development of proactive water quality management strategies and highlight the potential of advanced ML techniques in environmental monitoring.

Keywords: Ensemble Machine Learning, Algal bloom, Chlorophyll-a, Explainable AI, water quality.

Highlights:

- Chlorophyll-a concentration is predicted using machine and ensemble learning algorithms
- Ensemble learning algorithms tend to be more accurate than linear models
- Use of voting and stacking classifiers for fusion of multiple weak learners demonstrated
- XAI algorithm to determine the effect of input feature on model output
- SHAP to identify the most important factors on chlorophyll-a concentration prediction

Graphical Abstract:

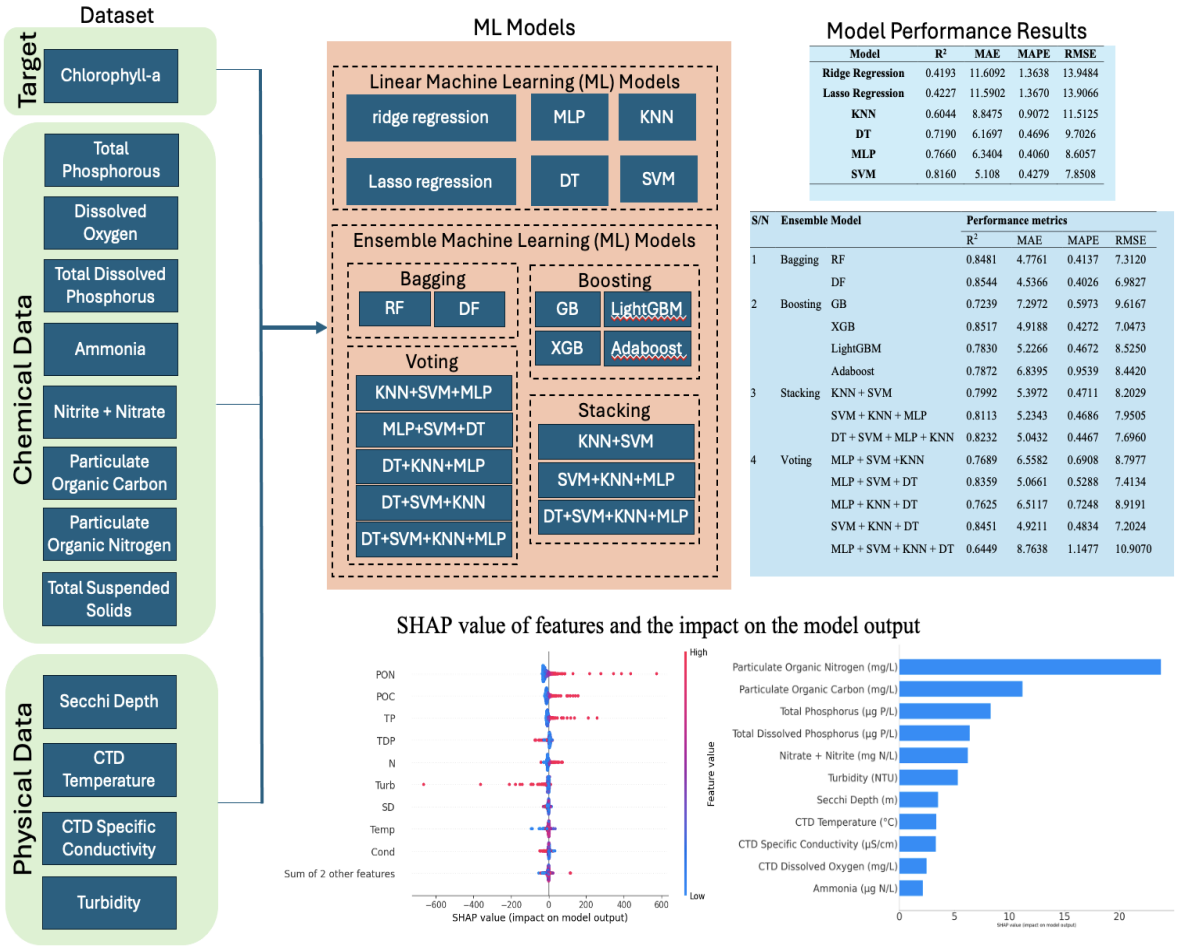

Model	R^2	MAE	MAPE	RMSE
Ridge Regression	0.4193	11.6092	1.3638	13.9484
Lasso Regression	0.4227	11.5902	1.3670	13.9066
KNN	0.6044	8.8475	0.9072	11.5125
DT	0.7190	6.1697	0.4696	9.7026
MLP	0.7660	6.3404	0.4060	8.6057
SVM	0.8160	5.108	0.4279	7.8508

S/N	Ensemble Model		Performance metrics			
			R^2	MAE	MAPE	RMSE
1	Bagging	RF	0.8481	4.7761	0.4137	7.3120
		DF	0.8544	4.5366	0.4026	6.9827
2	Boosting	GB	0.7239	7.2972	0.5973	9.6167
		XGB	0.8517	4.9188	0.4272	7.0473
		LightGBM	0.7830	5.2266	0.4672	8.5250
		Adaboost	0.7872	6.8395	0.9539	8.4420
3	Stacking	KNN + SVM	0.7992	5.3972	0.4711	8.2029
		SVM + KNN + MLP	0.8113	5.2343	0.4686	7.9505
		DT + SVM + MLP + KNN	0.8232	5.0432	0.4467	7.6960
4	Voting	MLP + SVM +KNN	0.7689	6.5582	0.6908	8.7977
		MLP + SVM + DT	0.8359	5.0661	0.5288	7.4134
		MLP + KNN + DT	0.7625	6.5117	0.7248	8.9191
		SVM + KNN + DT	0.8451	4.9211	0.4834	7.2024
		MLP + SVM + KNN + DT	0.6449	8.7638	1.1477	10.9070

1. Introduction

Environmental pollution has considerably elevated cyanobacterial biomass in aquatic systems, leading to degraded water quality all around the world. The increase in Harmful Algal Blooms (HABs), especially those involving cyanobacteria, has become a major global issue. The term "bloom" denotes the rapid proliferation of blue-green algae or cyanobacteria, which are hazardous due to the toxins they produce (Carmichael & Falconer, 1993). These blooms deteriorate water quality, threaten public health, and disrupt aquatic ecosystems, driven by nutrient pollution from agricultural runoff (Mount et al., 2024), industrial waste, and climate changes such as rising water temperatures (Paerl & Paul, 2012; Graham et al., 2016). HABs generate harmful toxins, impair waterway aesthetics, and complicate the provision of clean drinking water (Weirich & Miller, 2014).

Recent years have seen a sharp rise in HAB events due to population growth, agriculture (Yildirim and Demir, 2022), pollution, and climate change (Islam et al., 2024). This trend highlights the need to enhance HAB monitoring, modeling, and prediction to protect water resources and public health (Greene et al., 2021; Ratté-Fortin et al., 2023; Paerl et al., 2016; Yan et al., 2024). Direct measurement of algal concentrations is labor-intensive, so chlorophyll-a (Chl-a) is often used as a proxy for indicating algal blooms and water quality (Demiray et al., 2024; Boyer et al., 2009; Mellios et al., 2020). HAB formations often result from eutrophication, poor water quality (Yeşilköy & Demir, 2023), and climate change (Wells et al., 2015; Glibert, 2020; Zhou et al., 2022; Tanir et al., 2024).

Studies focusing on individual factors like nutrients, land use, or climate drivers often lead to oversimplified predictions (Wells et al., 2020; Maze et al., 2015; Paerl et al., 2011; Nourani et al., 2023). Effective HAB monitoring requires laboratory analysis of a variety of indicators like chlorophyll-a, cyanobacteria, and algal toxins (Katin et al., 2021; Giere et al., 2020; Greer et al., 2016) using techniques such as microscopy, spectrophotometry, liquid chromatography, and biochemical assays (Lombard et al., 2019). Remote sensing from satellites and UAVs provides valuable spatial data on HAB spread (Rolim et al., 2023; Kislik et al., 2022; Cheng et al., 2020; Qui et al., 2023). Addressing algal blooms requires understanding of their causes and implementing effective management strategies, including timely prediction of HABs to protect ecological and human health.

In recent decades, advanced machine learning (ML) algorithms have been employed to predict water quality (Bayar et al., 2009), including chlorophyll-a (Chl-a) concentrations (Park et al., 2022). Wu et al. (2014) used artificial neural networks (ANN) to predict daily Chl-a in a German lowland river by utilizing climate and water quality data as independent input variables. Similarly, Huang et al. (2015) employed ANN to predict monthly Chl-a in a lake. The support vector machine (SVM) is another ML algorithm used to predict water quality information, including total nitrogen, total phosphorus (TP), and Chl-a (Liu & Lu, 2014; Park et al., 2015).

Additionally, Derot et al. (2020) applied the Random Forest (RF) to predict cyanobacteria concentrations, while Busari et al. (2024) predicted Chl-a using RF, multilayer perceptron (MLP), support vector regression (SVR), and Jeong et al. (2022) used the RF and eXtreme Gradient Boosting (XGB) model to forecast algal blooms. Furthermore, Shin et al. (2021) used a variety of decision tree-based classifiers to forecast the occurrence of HABs in harmful bodies of water. Recently, Ai et al. (2023) used nine widely employed ML-based classification and

regression models such as the ANN, BA, RF, GB, and KNN for HAB prediction, demonstrating the capabilities of several models on algal bloom predictions.

Various tree-based ensemble algorithms have been applied to predict water quality information (Shin et al., 2020; Park et al., 2022). Ensemble ML models use a group of models composed of multiple weaker learners to enhance the accuracy of the final outcome or prediction of the final fused model, making it more accurate (Sutton, 2005). Random forests (RF) and gradient-boosted decision trees (GBDT) are commonly used tree-based ensemble models where decision tree models serve as weak learners. The XGB is among the popular and widely used GBDT models (Zhang et al., 2018; Jeong et al., 2022). Lin et al. (2024) also demonstrated the use of other ensemble ML algorithms such as the AdaBoost, LightGBM, and stacking regressor, in addition to other common ensemble ML algorithms. Despite their potential, these models face challenges such as the black-box nature of predictions, requiring explainable artificial intelligence (XAI) to enhance their interpretability and usability.

All the ML models previously discussed exhibit black-box characteristics. This means that the end user has access only to the input data and final prediction outputs by the models (Saeed & Omlin, 2020). Consequently, users are often unaware of the reasoning behind the predictions made by complex AI systems and algorithms. Recently, explainable artificial intelligence (XAI) has emerged to overcome the 'black-box' nature of ML models (Arrieta et al., 2020). Among the various explanation techniques, Shapley additive explanation (SHAP) is the most representative post hoc analysis technique (Lundberg & Lee, 2017).

SHAP can estimate the magnitude of the positive or negative contribution of the input features to a model's output (Lundberg et al., 2020). Additionally, SHAP is commonly utilized in the field of hydrology because it can effectively visualize the importance and effect of various factors on water quality. For example, Cha et al. (2021) estimated the contributions of environmental factors on species distributions, while Kim et al. (2022) analyzed spectral bands on satellite images to predict Chl-a values in lake water. Finally, Jeong et al. (2022) identified relative water quality feature importance in HAB predictions using SHAP.

Grasping the underlying factors of HAB is critical for informing public and decision-makers (Xu et al., 2020), as it empowers them to make informed interventions and policy decisions based on a transparent understanding of the causes and dynamics of harmful algal blooms (Weber et al., 2018). Communicating these insights through novel information and communication systems and technologies (Demir et al., 2009), such as virtual reality, can further enhance understanding by providing immersive and interactive experiences (Sermet and Demir, 2022) that vividly illustrate complex data and predictive outcomes.

Lake Erie, part of the Great Lakes system, serves as a critical case study for examining HABs. The Great Lakes constitute the largest and most biodiverse freshwater reserve on Earth (Magnuson et al., 1997; Tewari et al., 2022). The basin encompasses both industrial facilities focused on manufacturing and areas dedicated to agriculture. Lake Erie is the shallowest and smallest lake in terms of water volume, but the fourth largest in terms of area. It is ecologically, culturally, and economically significant to the approximately 12.5 million people who live in its watershed. Each year Lake Erie supports nearly 14,000 ton in harvested fish, over 33 million tons of transferred cargo, and over 1.5 million dollars in recreational businesses (Sterner et al., 2020).

However, it experiences significant challenges from nutrient overload, especially in its western basin due to its geographical location (Boegehold et al., 2023). Since 2002, Chl-a concentration, a commonly used indicator of potential upcoming HABs, has dramatically increased annually in Lake Erie, reaching unprecedented levels in recent years (Stumpf et al., 2016; Boegehold et al., 2023). Humans can be exposed to harmful algae through ingestion of contaminated fish and drinking water and inhalation and dermal exposure during recreational events such as swimming and boating (Carmichael and Boyer, 2016; Buratti et al., 2017). Given the potential threats HABs pose to humans, the economy, and the environment, accurate prediction of HAB occurrences is essential. Identifying key factors influencing these blooms is crucial for implementing preventive measures to mitigate potential losses (Kouakou and Poder, 2019).

Despite the increasing prevalence of SHAP in hydrology, there is still limited research on it in the field of HABs (Park et al., 2022; Baydaroglu et al., 2024). Previous studies surrounding Lake Erie have mainly focused on field measurements, statistical methods, machine learning techniques to predict HABs. Additionally, existing research has only focused on HAB prediction performance, meaning few studies have identified the effect of each variable on predicted chlorophyll-a values. Therefore, this paper aims to assess the capabilities of SHAP on determining the effect of various water quality data input features. Ensemble-based ML models are also examined using SHAP to further advance the algal alert system by identifying the most important indicators of a potential HAB in Lake Erie.

The objectives of this study are to (1) utilize extensive datasets that include physical, chemical, and biological water quality parameters from multiple monitoring stations; (2) predict the occurrence of HABs using ensemble-based ML models; and (3) identify relative feature importance in HAB occurrence predictions using SHAP. This paper is structured as follows: Section 2 describes the methodology, including data collection and ensemble-based ML model implementation. Section 3 presents the results and discussion, highlighting the effectiveness of SHAP in interpreting the models. Section 4 concludes with insights into the implications of the findings and suggestions for future research.

2. Methodology

2.1. Study Area

In this study, we used water quality data collected from 7 monitoring stations (Fig. 1) by National Oceanic and Atmospheric Administration (NOAA) Great Lakes Environmental Research Laboratory (GLERL) on the Western side of Lake Erie. This dataset includes water quality measurements from 2013 to 2020 (Boegehold et al., 2023). These stations are selected to represent different nutrient, sediment and hydrologic inputs into the western basin of Lake Erie and are located in areas consistently susceptible to HABs.

Based on the available data, we selected physical, chemical and biological variables, shown in Table 1, as representative input features and chlorophyll-a as the target (output) feature for machine learning modeling. Physical variables include secchi depth, ctd temperature, ctd specific conductivity, and turbidity. Chemical drivers also include ctd dissolved oxygen, total phosphorus, total dissolved phosphorus, ammonia, nitrate + nitrite, particulate organic carbon, particulate organic nitrogen, and total suspended solids.

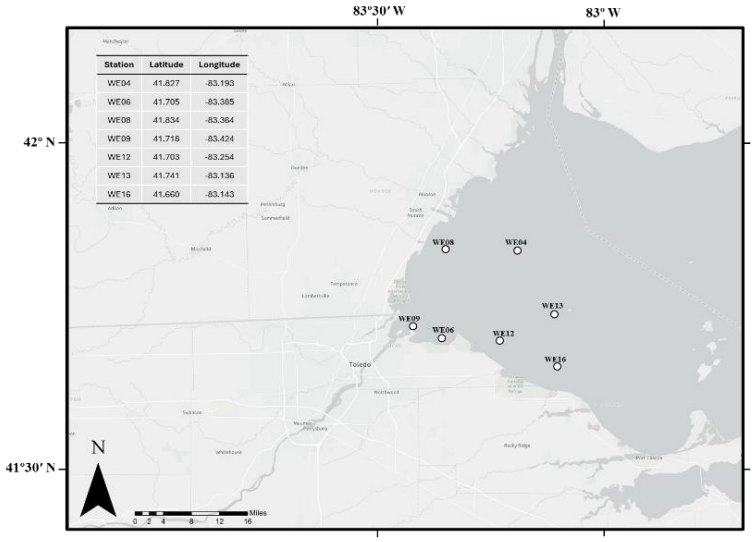

Figure 1. Location of water quality monitoring stations in Lake Erie

Table 1. Summary of the output (dependent variable) and input features (independent variables) for HABs prediction.

Variable	**Abbreviation**	**Unit**	**Definition**
Secchi Depth	SD	m	Penetration depth of sunlight through the water
CTD Temperature	T	°C	Water temperature at site
CTD Specific Conductivity	Cond	µS/cm	Conductivity value of water at site
CTD Dissolved Oxygen	DO	mg/L	Concentration of dissolved oxygen at site
Turbidity	Turb	NTU	Cloudiness of fluid caused by suspended solids
Total Phosphorus	TP	µg/L	Concentration of the sum of all phosphorus compounds that occur in various forms at site
Total Dissolved Phosphorus	TDP	µg /L	Concentration of the portion of phosphorus that is dissolved at site
Ammonia	A	µg /L	Concentration of Ammonia at site
Nitrate + Nitrite	N		Concentration of NO_x at site
Particulate Organic Carbon	POC	mg/L	Concentration of organic carbon particles suspended in water at site
Particulate Organic Nitrogen	PON	mg/L	Concentration of organic nitrogen particles suspended in water at site
Total Suspended Solids	TSS	mg/L	Concentration of both organic and inorganic particles suspended in water at site
Chlorophyll-a	Chll-a	µg /L	Indicator of HABs

Figure 2 shows the average Chlorophyll-a concentrations at seven stations in Lake Erie, spanning from 2013 to 2020. The data is presented on a monthly scale, with distinct bars representing the average concentrations for each month from May through October. The figure provides valuable insight into the temporal dynamics of algal blooms in Lake Erie, highlighting

both seasonal and interannual variations in Chl-a concentrations. The peak in August for several years suggests that monitoring efforts during late summer are crucial for understanding and managing HABs. Additionally, the marked variability between years underscores the need for continuous monitoring to capture the complex interplay of factors driving algal blooms in the lake.

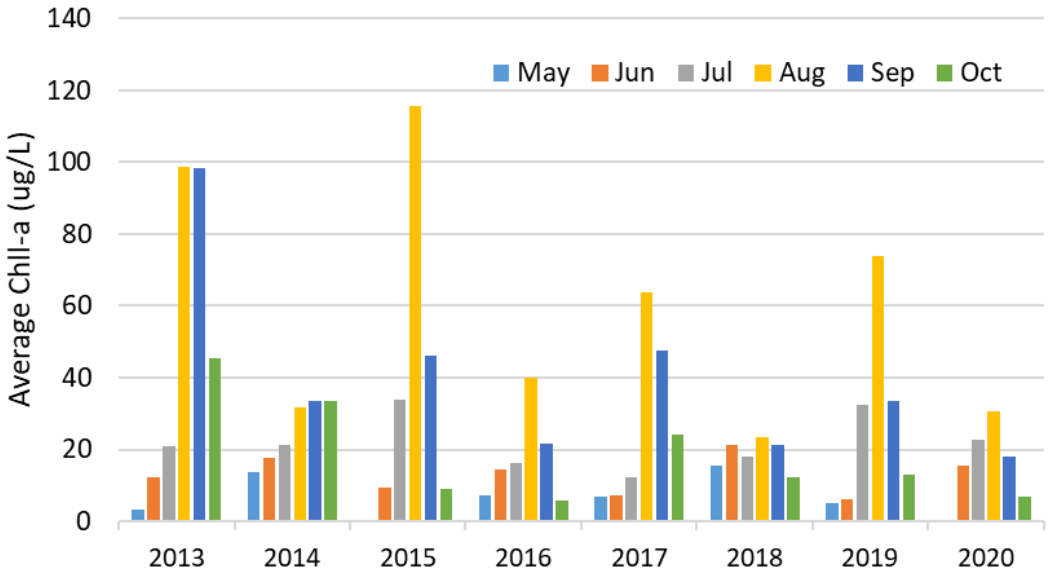

Figure 2. Monthly average Chlorophyll-a (Chl-a) concentrations (µg/L) measured at seven stations in Lake Erie from 2013 to 2020.

2.2. Machine Learning Models

The linear models selected are Ridge and Lasso regression, SVM, MLP, DT, and KNN. Each of these models has been proven to be well suited for all sorts of regression tasks, including for predicting algae blooms. These models are compared based on their performance and are also tested for their efficiency since real-time forecasting is also highly important.

Linear Regression: The ridge and lasso regression methods are two commonly used linear regression methods developed for a variety of forecasting tasks. Ridge regression works through using a parameter estimation method to reduce the effect of collinearity, a common problem which occurs when there is a high correlation between two variables. Through reducing collinearity, it will increase the reliability of a regression model. The ridge regression method also has the capability of penalizing outliers in data, which further helps to create an accurate linear regression model.

Thus, ridge regression has been commonly applied in a wide variety of tasks ranging from genetic studies to finance (Arashi et al., 2021; Pereira et al., 2016). Lasso regression is also an extension of the ordinary least squares method, and it reduces error by shrinking some coefficients of features to zero to find the most optimal method (Ranstam and Cook, 2018). By doing so, lasso regression can select features more accurately. Finally, lasso regression also utilizes the L1 regularization method, which introduces another penalty using the absolute value of coefficients. This method has been applied for rainfall modeling (Sari, 2021) and both models have proven to have some success when dealing with regression tasks.

Multi-Layer Perception (MLP): The multi-layer perceptron (MLP) is a deep neural network algorithm capable of performing both classification and regression tasks which also adapts well to linear and nonlinear data. It contains three main layers: the input layer, the hidden layers, and the output layers. The hidden layers are all fully connected with each other and contain an activation function which transports inputs to outputs. Each layer contains a different number of perceptrons, which make the calculations in the model. The perceptron uses a weighted average method to mimic the neurons in a human brain, and if that certain weighted average exceeds a certain threshold, then that information is passed to other perceptrons. The MLP has been successful at a wide variety of tasks including in predicting chlorophyll-a values (Sammartino et al., 2020).

Support Vector Machine (SVM): The support vector machine is another commonly used machine learning method which maps points in a higher dimensional space to a hyperplane, which allows it to categorize data of high dimensions by splitting the data up into multiple different groups (Yu and Kim, 2012). To find the hyperplane, a kernel, which transforms data to the required form, can be utilized without increasing the computation cost. In regression tasks, a similar method is used, except hyperplanes represent a best fit line with a threshold value between decision boundaries. Through doing so, it is also commonly used in regression tasks such as algae blooms, and it is relatively memory efficient compared to other models (Wang et al., 2017).

Decision Trees: Decision trees are a popular machine learning algorithm which can be used in both classification and regression tasks (Quinlan, 1986). The key features of the decision tree are splitting and pruning. Splitting in a decision tree works by dividing the dataset into subsets based on the value of the selected feature, and the process is repeated recursively to build the tree. A decision tree is built through various nodes with each node representing a decision a result of a question, and the leaf nodes representing a value that comes as a result of that decision. Each additional branch that is added to a decision tree is another possible route that can be taken in the decision tree to reach a final solution. Another part of the decision tree is pruning. Pruning works to reduce overfitting in decision trees by removing any unnecessary branches or nodes since decision trees are traditionally significantly impacted by noisy data. Decision trees have recently been applied to form new ensemble algorithms (i.e. Random Forest) and other classification and regression tasks (Liaw and Wiener, 2002).

K-Nearest Neighbors (KNN): The KNN is a commonly used machine learning algorithm that works by categorizing data points with similar values (Guo et al., 2003). The tuning of the parameter of the K nearest neighbors is utilized to make predictions, with a smaller K leading to noisy predictions while a larger K leads to the overfitting of the model. The K nearest neighbors to a certain data point are determined based on a distance metric which computes the distance between every data point in a dataset, where the distance metric used is often dependent on the dataset itself. Then, for regression tasks, the algorithm averages the values of the K nearest neighbors for the final prediction after calculating the distance between that point and other points. The KNN has been used successfully in algae bloom predictions in previous works (Jung et al., 2010; Wang et al., 2021).

2.3. Ensemble Learning Models

Ensemble learning is a machine learning method where multiple different learners are fused together to form a large model. This technique is especially important in environmental engineering because it helps reduce uncertainty in models and improve redundancy and accuracy. The ensemble methods can be split into four main categories: bagging, boosting, voting, and stacking. The detailed algorithms are further discussed below.

Bagging Algorithms

Random Forest (RF): The random forest is a bagging ensemble method based on the ensemble of multiple different decision trees, where the combination of multiple weak learners and decision trees will increase model performance (Breiman, 2001). Bagging uses bootstrapping, where models are trained on subsets of a dataset and the final predictions from each model are fused together. The split of a node in a tree relies on random subsets of features, and this is continued until the entire tree is built. The key features of the random forest are its diversity and robustness since each model is trained on a separate section of data, and the random forest can be easily scaled to larger datasets. However, the algorithm is sensitive to noisy data, since it is not distributed evenly, and the individual decision trees must be sufficiently deep. Thus, the random forest can handle continuous variables, making them suitable for regression tasks. The random forest is one of the most utilized machine learning algorithms in multiple domains including algae bloom prediction.

Deep Forest (DF): The deep forest (DF) is a novel method developed by Zhou et al. (2019) which utilizes the stacking ensemble method through a cascade structure, implementing deep learning with ensemble learning. The final structure is similar to that of a neural network, but instead of neurons, layers of random forests are built. A sliding window is used to scan the raw features in the deep forest. Each layer of the deep forest contains multiple random forests as learners. The algorithm takes inspiration from stacking ensemble methods, where using an abundance of weaker learners for a fully ensemble algorithm is an important concept. Thus, model diversity plays a key role in stacking algorithms, and the deep forest emphasizes that concept through having each model search through different subsets of the training dataset. Moreover, the deep forest is also ideal for training since it requires a small number of hyperparameters. This novel method has had limited applications, especially in the field of environmental science and algae blooms.

Boosting Algorithms

Gradient Boosting (GB): The gradient boosting algorithm is another decision tree-based model, but it utilizes the boosting technique in ensemble learning (Friedman, 2001). The boosting technique is where a model is trained initially, and a second model is trained based on the errors of the first model. Each tree in the gradient boosting algorithm is built sequentially instead of independently, and so each tree is fitted to the errors of previous predictions. Through each iteration, the weights in the model are adjusted to improve performance. Then, the gradient descent in the model optimizes loss by decreasing it as much as possible when new weaker learners are added to the full model throughout the training process. The gradient boosting algorithm is used as a method of fusion for the individual models.

Extreme Gradient Boosting (XGBoost): The Extreme Gradient Boosting algorithm is an extension of the gradient boosting algorithm which reduces overfitting during training using regularization penalties (Chen and Guestrin, 2016). Similarly to the gradient boosting

algorithm, the XGBoost sequentially and iteratively adds learners such as decision trees to a model, and newer learners would focus on the errors from previous learners. However, the main difference between the XGBoost and standard gradient boosting is that it uses enhanced regularization techniques, improving the generalization capabilities of the model. The XGBoost is also highly efficient, even across larger datasets. Recently, the XGBoost has been applied to a variety of fields from diabetes detection (Prabha et al., 2021) to algae bloom prediction (Ghatkar, et al., 2019). This algorithm is also used for the fusion of multiple other models in this study.

Light Gradient Boosting (LightGBM): The Light Gradient Boosting algorithm is another commonly applied gradient boosting method in machine learning (Ke et al., 2017). First, data is split into different bins of multiple data points instead of individual data points, allowing training times to decrease. Like the other gradient boosting algorithms, the LightGBM iteratively adds learners to an ensemble of decision trees. However, the key difference is that LightGBM builds its tree leaf-wise rather than depth-wise to achieve lower loss and improve efficiency, allowing it to be faster than the XGBoost. Finally, LightGBM uses gradient one-sided sampling in order to focus on data points with a higher prediction error. The LightGBM is used as an individual model in this study and has been applied in the past mainly for tasks which require high efficiency.

Adaptive Boosting Algorithm (Adaboost): The Adaboost, or adaptive boosting algorithm, is an ensemble algorithm which combines multiple weaker learners into one strong learner. A weak learner is a classifier that performs only slightly better than random guessing, and Adaboost starts by training multiple of these learners on weighted versions of training data. First, all samples in a dataset are assigned the same weight. The Adaboost uses the boosting method through iteratively focusing on incorrect predictions from the model and improving them accordingly. After the training process, new weights are assigned to each classifier based on their accuracy. Finally, every weak learner is combined and normalized to make the final output or prediction. The Adaboost algorithm has seen usage in medical fields among many others (Hatwell et al., 2020).

Voting Algorithms:

The voting classifier is another type of ensemble learning method which combines the predictions of multiple individual classifiers to improve performance (Bauer and Kohavi, 1999). It can fuse multiple different methods and models, and it takes a weighted average of all different inputs. These weights can be trained and fitted based on the input data. The main advantage of the voting classifier is that it has improved generalization performance than individual models. There are two main types of voting used in the voting classifier: hard voting and soft voting. Hard voting is where the instance with the most votes is the final output, while soft voting, which is implemented in this research, uses a weighted average and is more suitable towards regression tasks.

Stacking Algorithms:

Stacking is another ensemble method of combining the predictions of individual classifiers (Wolpert, 1992). The key difference between stacking and voting is that it uses a final estimator, which interprets the meta-features of several base estimators trained on the original dataset. Thus, during the prediction process, each individual base estimator first makes its prediction, and the final estimator combines the results of these several models to make the

final prediction. One advantage of stacking is that a variety of diverse models can be fused, which helps improve the robustness and accuracy of the method. Recently, stacking ensembles have been applied and are successful at predicting algal blooms with improved accuracy (Ly et al., 2023).

2.4. Model Development

Figure 3 presents a comprehensive workflow diagram for a ML based HAB prediction. As shown in the figure, the initial step in the workflow involves obtaining water quality data from seven different stations located on the western basin of Lake Erie and operated by Great Lakes Environmental Research Laboratory (GLERL), NOAA. The presence of unordered, raw, missing, or duplicate instances in the dataset can lead to inaccuracies in system predictions, making data preprocessing essential. Subsequently, the organized data are split into training and testing samples, where the chosen ML models are trained using the training sample (cover 2013 to 2019), and testing samples (2020) are employed to observe the behavior of the trained models.

This would allow each model to demonstrate their performance in predicting yearly chlorophyll-a values. Since our dataset contains many more samples than features, we were careful not to reduce the number of features too much to avoid losing important information. This strategy helps us balance capturing a wide range of influencing factors and maintaining the robustness of our model. The min-max method (MinMaxScaler) was applied to standardize the features to eliminate potential model bias due to difference in scales and units (Ahsan et al., 2021). The min-max method transforms the data into a range 0 and 1 and ensures that all features contribute equally to the model by bringing them to a common scale, which helps improve the performance of machine learning algorithms.

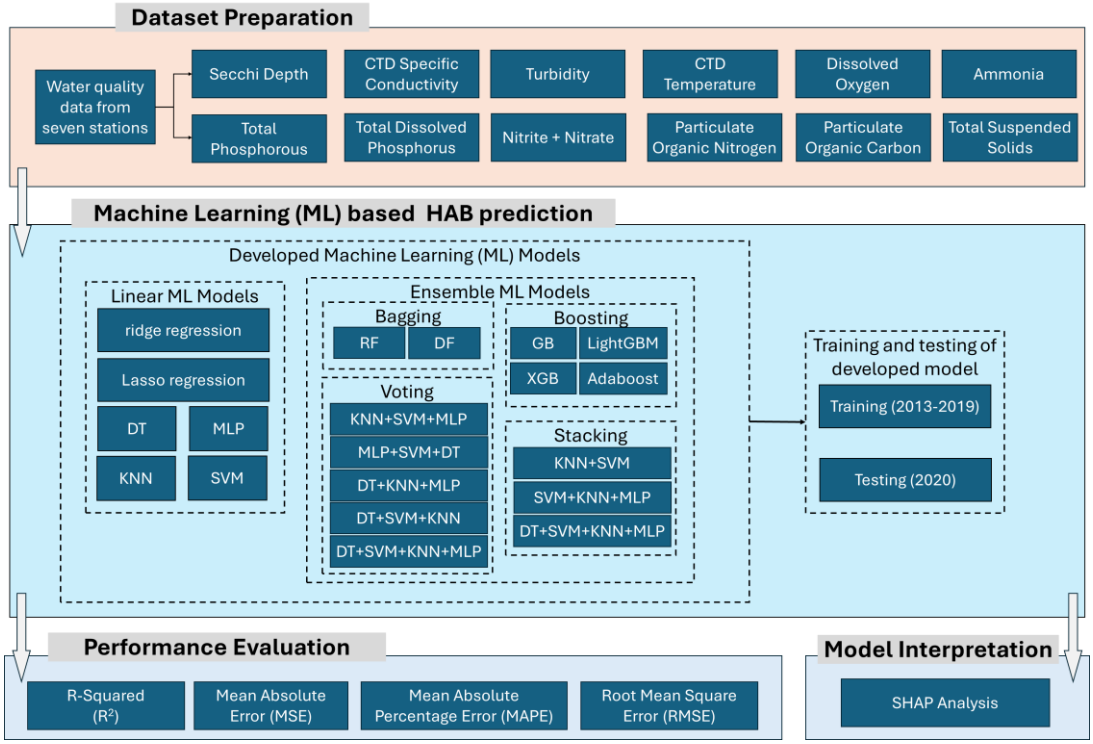

Figure 3. Workflow diagram for all scenarios in HABs prediction.

A variety of ML models are then developed and tested to predict chlorophyll-a concentrations. Table 2 lists the training parameters for each of the selected ML models used for HAB prediction in this study. The tuning of these hyperparameters was achieved through cross validation, where the performance of models under different parameters would be evaluated until the most accurate model setting was determined. Various combinations of individual ML models were evaluated for ensemble modeling. For the voting and stacking classifiers, different combinations of two to four linear ML models were tested. These models included SVM, MLP, KNN, and DT, as they all achieved R^2 values above 0.5 but showed significant variation among themselves. Therefore, different combinations of these models were explored to assess the impact on accuracy when combining stronger and weaker learners.

Table 2. Summary of training parameters of models developed in this study

Models	**Parameters**
Ridge Regression	Alpha = 100
Lasso Regression	Alpha = 100
KNN	N_neighbors = 30
DT	Min_samples_split = 2, min_samples_leaf = 1
MLP	Epochs = 2000, learning rate = 0.001, batch size = 32
SVM	Kernel = rbf, c = 100000
LightGBM	Leaves: 31, learning_rate: 0.05, rounds: 100, feature_fraction: 0.9
RF	N_estimators = 1000
AdaBoost	N_estimators = 100, learning_rate = 0.1
DFC	N_estimators = 50
GB	N_estimators = 1000
XGBoost	Num_rounds = 100

Following the acquisition of results for selected evaluation parameters and model performance are analyzed and compared. Finally, model interpretation utilizes SHAP analysis to provide insights into the contribution of each feature within the dataset to the model's predictions. This analysis aids in understanding the underlying factors driving the model's output, ensuring transparency and interpretability of the results.

2.5. Model Evaluation

We calculated the values of R-squared (R^2), mean absolute error (MSE), mean absolute percentage error (MAPE) and root mean square error (RMSE) for evaluating the model performance, which are widely accepted metrics. These metrics have been extensively applied in HAB prediction research due to their interpretability and ability to capture different aspects of model performance.

R^2 indicates how well the predictive value explains the measured value. In this work, measured and predicted chlorophyll-a concentrations were taken as the dependent and independent variables respectively, and the R^2 was determined by applying linear regression analysis. The R^2 values range from 0 to 1, with higher values indicating a higher prediction accuracy. The formula for R^2 is shown as follows:

$$R^2 = 1 - \frac{\sum_{i=1}^{n}(y_i - \hat{y_i})^2}{\sum_{i=1}^{n}(y_i - \bar{y})^2} \quad \text{Eq. 1}$$

where y_i is the i^{th} actual value and $\hat{y}$ is the i^{th} predicted value of the dependent variable, and $\bar{y}$ is the mean of y_i.

Root mean square error (RMSE), which indicates the mean error between the predicted and measured values, is one of the most widely used performance indicators to express the general performance of prediction model (Sit et al., 2024). In this study, we calculated the mean error between the measured chlorophyll-a concentration and that predicted by the model. The equation is given below; the lower the RMSE values; the higher the prediction performance of the model. y_i is the i^{th} actual value and $\hat{y_i}$ is the i^{th} predicted value of the dependent variable, and n is the number data points.

$$RMSE = \sqrt{\frac{1}{n}\sum_{i=1}^{n}(y_i - \hat{y_i})^2} \quad \text{Eq. 2}$$

Mean absolute error (MAE) is also a widely used performance metric to provide an intuitive and easily interpretable measure of prediction model performance (Jiang et al., 2022). The mean absolute error between the measured and predicted chlorophyll-a concentrations were computed without considering their directions. A lower MAE indicates a better model fit, showing that the model's predictions are closer to the true values. It is also beneficial when comparing different models on the same dataset, as it can help identify the model with the most accurate predictions.

$$MAE = \frac{1}{n}\sum_{i=1}^{n}|(y_i - \hat{y_i})| \quad \text{Eq. 3}$$

Mean absolute percentage error (MAPE) is also widely used to interpret model performance model performance (Yan et al., 2024). It emphasizes smaller relative errors, and it does not based on different scaling of the input feature variables. Smaller MAPE value indicate enhanced accuracy and stronger predictive capabilities of the model.

$$MAPE = \frac{1}{n}\sum_{i=1}^{n}\left|\left(\frac{y_i - \hat{y_i}}{y_i}\right)\right| \times 100\% \quad \text{Eq. 4}$$

2.6. Model Interpretation Using XAI

The effects of the water quality parameters on the HAB prediction were explained using the SHAP method. SHapley Additive exPlanations (SHAP) which is a post-hoc and model-agnostic technique, unifies multiple interpretability methods under the concept of Shapley values (Lundberg et al., 2020; Stubblefield et al., 2020). It establishes a new explanatory model, for a given black-box system, by uncovering associations between the feature values and the

output of the black-box system (Burkart and Huber, 2021). This method is based on coalitional game theory and Shapley values, a unique distribution (among the players) of the total surplus generated by a coalition of all players in a cooperative game (Lundberg and Lee, 2017).

In this study, TreeSHAP was used to estimate the SHAP value which represents the importance of the input variables in predicting the results using machine learning models. The 'shap.TreeExplainer' function enabled us to plot feature importance for global explainability, facilitating a better understanding of decision-making within our models. This analysis compensates for the black-box type shortcomings of the machine learning model and indicates the extent to which each variable affects the objective variable after entering the model.

3. Results and Discussions

3.1. Individual ML Model

The performance metrics of various individual ML models, as summarized in Table 3, highlight the effectiveness of different linear machine learning models in terms of their predictive accuracy and error rates. R^2, or the coefficient of determination, measures the proportion of variance in Chl-a concentrations that is predictable from the independent variables. Higher R^2 values indicate better model performance. According to the observed R^2 in the table, the SVM stands out with the highest R^2 of 0.816, indicating that it explains approximately 82% of the variance in Chl-a concentrations, making it the most predictive model among those evaluated.

MAE and RMSE are both measures of prediction error, with MAE representing the average absolute error and RMSE providing a measure that penalizes larger errors more than MAE. Lower values for both metrics are preferred as they indicate higher accuracy. The SVM, with the lowest MAE of 5.108 and RMSE of 7.8508, suggests that its predictions are closest to the actual in Chl-a concentrations, and it handles larger errors better than the other models. MAPE, which indicates the average percentage error between predicted and actual values, further supports this by showing the SVM's effectiveness with a relatively low value of 0.4279.

Comparatively, Ridge and Lasso Regression models, with R^2 values around 0.42 and higher MAE and RMSE values, demonstrate moderate performance, making them less preferable for high-accuracy requirements in Chl-a prediction. The KNN model improves upon these, but the DT and MLP models offer substantial improvements, as evidenced by their higher R^2 values and lower error metrics.

Table 3. Summary of performance metrics of linear ML models

Model	R^2	MAE	MAPE	RMSE
Ridge Regression	0.4193	11.6092	1.3638	13.9484
Lasso Regression	0.4227	11.5902	1.3670	13.9066
KNN	0.6044	8.8475	0.9072	11.5125
DT	0.7190	6.1697	0.4696	9.7026
MLP	0.7660	6.3404	0.4060	8.6057
SVM	0.8160	5.108	0.4279	7.8508

3.2. Ensemble ML Models

Table 4 presents a comprehensive summary of the performance metrics for various ensemble models used to predict chlorophyll-a values. In the bagging category, both the RF and DF

exhibit strong predictive performance. The DF model slightly outperforms the RF model, achieving an R^2 of 0.8544 compared to RF's 0.8481. Additionally, DF has a lower MAE (4.5366) and RMSE (6.9827), indicating better accuracy and lower prediction error than the RF, which has an MAE of 4.7761 and an RMSE of 7.312. The MAPE values also show that DF (0.4026) provides more precise predictions than RF (0.4137).

Among the boosting models, XGB stands out as the top performer, with an R^2 of 0.8517, surpassing the other boosting models like GB, LightGBM, and AdaBoost. XGB also has a lower MAE (4.9188) and RMSE (7.0473) compared to GB, which has a notably lower R^2 of 0.7239 and a higher MAE (7.2972) and RMSE (9.6167). LightGBM and AdaBoost show moderate performance, with LightGBM having an R^2 of 0.7830 and AdaBoost having an R^2 of 0.7872, though both have higher MAE and RMSE values compared to XGB.

In this study, stacking models were developed using the KNN algorithm as a meta-learning model because it does not require much training and can handle both continuous and discrete data. Models with highest an R^2 score were chosen and paired with a KNN and based on the results obtained we realized that combining a strong model with KNN increases its R^2 value. The combination of DT, SVM, MLP, and KNN performs well, achieving an R^2 of 0.8232, compared to the other combinations. We also developed the same combinations with Lasso and Ridge regression as a meta-learning instead of KNN and observed similar performance metrics. We then decided to pair a strong model with a weak model and realized an increase in predictive performance.

Table 4. Summary of performance metrics for ensemble models

S/N	Ensemble Group	Ensemble Model	Performance Metrics			
			R^2	MAE	MAPE	RMSE
1	Bagging	RF	0.8481	4.7761	0.4137	7.3120
		DF	0.8544	4.5366	0.4026	6.9827
2	Boosting	GB	0.7239	7.2972	0.5973	9.6167
		XGB	0.8517	4.9188	0.4272	7.0473
		LightGBM	0.7830	5.2266	0.4672	8.5250
		Adaboost	0.7872	6.8395	0.9539	8.4420
3	Stacking	S#1 (KNN + SVM)	0.7992	5.3972	0.4711	8.2029
		S#2 (SVM + KNN + MLP)	0.8113	5.2343	0.4686	7.9505
		S#3 (DT + SVM + MLP + KNN)	0.8232	5.0432	0.4467	7.6960
4	Voting	V#1 (MLP + SVM +KNN)	0.7689	6.5582	0.6908	8.7977
		V#2 (MLP + SVM + DT)	0.8359	5.0661	0.5288	7.4134
		V#3 (MLP + KNN + DT)	0.7625	6.5117	0.7248	8.9191
		V#4 (SVM + KNN + DT)	0.8451	4.9211	0.4834	7.2024
		V#5 (MLP + SVM + KNN + DT)	0.6449	8.7638	1.1477	10.9070

Voting ensembles display mixed results, with some combinations performing significantly better than others. The ensemble of SVM, KNN, and DT achieves a high R^2 of 0.8451, with an MAE of 4.9211 and an RMSE of 7.2024, showing its effectiveness. In contrast, the ensemble

including MLP, SVM, KNN, and DT underperforms with a lower R^2 of 0.6449 and higher errors (MAE of 8.7638 and RMSE of 10.9070), suggesting that adding more models to the voting ensemble does not necessarily improve performance and can sometimes lead to worse results. In this case, we observed that any combination of any model with strong model increases its predictive performance.

The Figure 4 presents a detailed comparison of the performance of the best ensemble ML models (DF, XGB, S#3, and V#4) corresponding to each subcategory—bagging, boosting, voting and stacking—across different data subsets. The figure is organized into four rows, each dedicated to the best performing ensemble ML models, and within each row, three scatter plots are displayed. The columns represent the different data subsets used for evaluation. The first column corresponds to the model's performance on the training data, the second column corresponds to the model's performance on the test data, and the third column corresponds to the model's performance on the combined dataset (training and test data together).

In each plot, the x-axis represents the observed values, while the y-axis represents the predicted values by the model. The solid red diagonal line labeled "Perfect Fit" illustrates the ideal scenario where the model's predictions perfectly match the observed values. The blue dots (scatter points) show the actual data points, while dotted blue line represents the best linear fitting regression line between the observed and predicted values. The scatter points reveal the accuracy of the predictions, with deviations from the red line indicating prediction errors. The closer the scatter points cluster around the perfect fit line, the better the model's predictive accuracy.

The scatter plots for the S#3 stacking model combination reveal that while this stacking model can capture the overall trend of the data, there is a noticeable degree of scatter, particularly at higher concentration values for all subsets of data. This suggests that the S#3 may struggle with predicting extreme values accurately, leading to under estimation in those cases. The voting combination (V#4) shows a slightly improved performance compared to the S#3, with a tighter clustering of data points around the 1:1 line, particularly at moderate concentration levels and using test data. However, similar to the S#3, the V#4 combination also exhibits challenges in accurately predicting the highest concentrations, as indicated by the scatter and deviation of the regression line from the 1:1 line. The XGB and DF ensemble models demonstrate a distinct performance pattern compared to stacking and voting combinations. The scatter plots indicate that the XGB may better handle the variability in the data, as evidenced by a closer alignment of the points with the 1:1 line, particularly at higher concentrations.

This suggests that the XGB ensemble model might be more robust in capturing the complex relationships in the dataset, leading to more accurate predictions across the full range of observed chlorophyll-a concentrations. The results suggest that interpretable ensemble-based ML models have high applicability as decision-making tools to support the establishment of effective management strategies and are expected to provide decision-support data to establish effective water quality management strategies.

Overall, Table 3 highlights ensemble models, particularly those using bagging and boosting techniques, tend to achieve higher predictive accuracy for chlorophyll-a values. The DF and XGB models emerge as top performers in their respective categories, offering the best balance of high R^2 and low error metrics. Stacking and voting ensembles also demonstrate potential,

especially when optimally combining complementary models, but their performance can vary widely based on the specific combination of strong and weak models used.

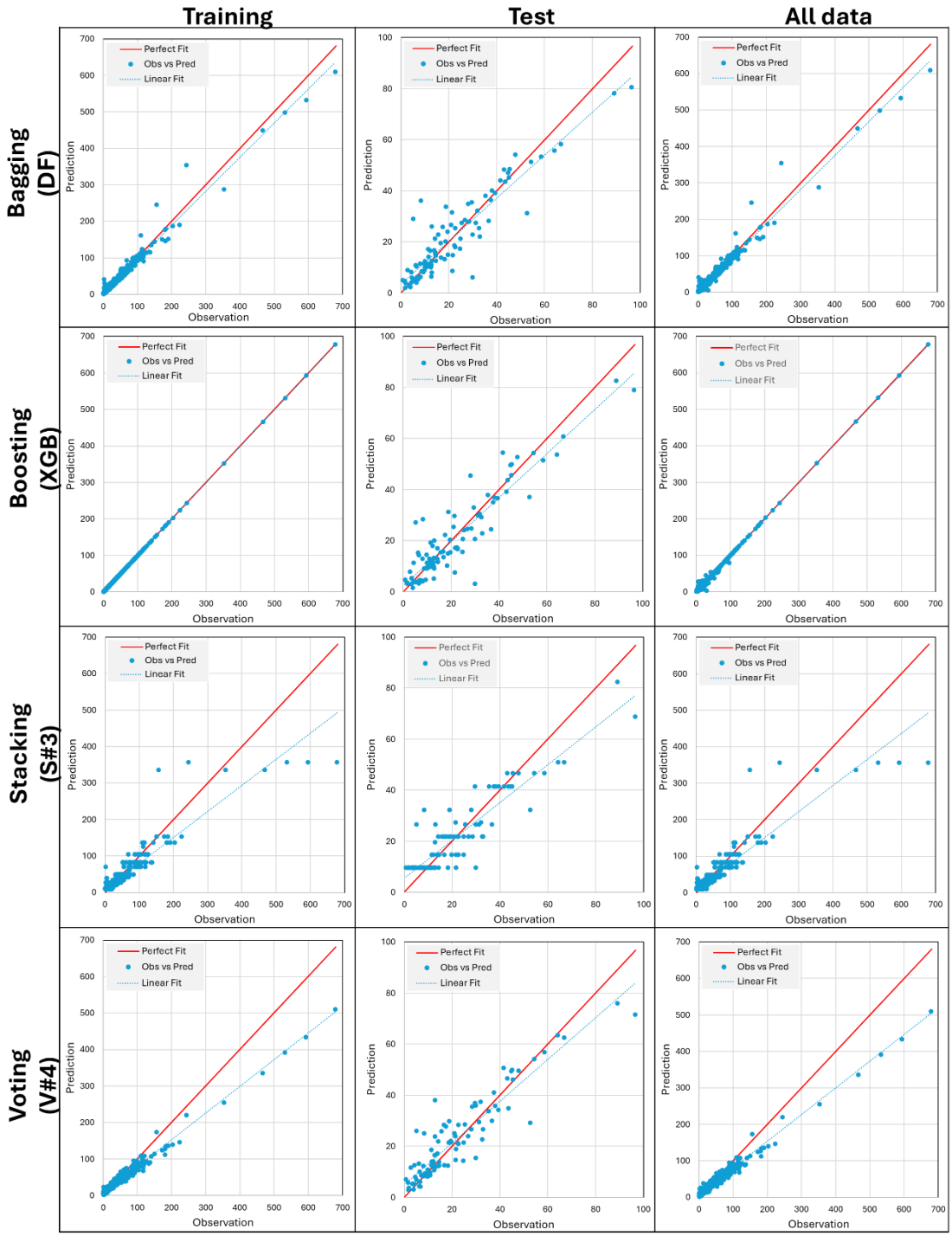

Figure 4. Scatter density plots of actual chlorophyll-a concentration (x-axis) versus prediction chlorophyll-a concentration (y-axis) by using the best ensemble ML models including bagging, boosting, voting and stacking.

3.3. Effect on Training Time and Model Performance

Table 5 summarizes the training times (in seconds) for various ensemble and individual ML models used to predict chlorophyll-a values. These times highlight each model's computational

efficiency, which is crucial for real-time or resource-constrained applications. The kNN model is the fastest, with a training time of just 0.5 seconds, followed by Lasso, Ridge, GB, and XGB, each taking 1 second, making them suitable for scenarios requiring quick model updates. More complex models like MLP and DF require significantly longer training times due to their complexity, with DF taking 561.8 seconds. Despite its long training time, DF delivers excellent predictive performance (R^2 = 0.8544), justifying the longer training in accuracy-critical applications. XGB stands out for combining both efficiency and performance, with a training time of 1.0 second and strong predictive metrics (R^2 = 0.8517), making it an attractive option for applications needing both high accuracy and low computational cost. The RF model, with a training time of 5.2 seconds, also strikes a good balance between performance and efficiency (R^2 = 0.8481). In time-sensitive scenarios, the choice of model should consider the trade-off between computational efficiency and predictive performance.

Table 5. Training times of each optimized model in seconds

Model	Training Runtime
Lasso	1.0s
Ridge	1.0s
MLP	144.9s
RF	5.2s
LightGBM	7.0s
SVM	12.7s
Adaboost	5.2s
DT	1.0s
KNN	0.5s
DF	561.8s
GB	1.0s
XGBoost	1.0s

3.4. SHAP Analysis-Interpreting Model Performance

In this study, we utilized the SHAP to analyze relative importance of the input features within various ML models for predicting HABs. The relative importance values (i.e., the mean |SHAP| value) provide insights into the contribution of each feature to the model's predictions, enabling us to understand the driving factors behind the predictions. Table 6 presents the mean |SHAP| values of the five most important input features in each ML model used in our study. Our finding indicates that in the western part of Lake Erie, Chl-a concentration is primarily influenced by the Particulate Organic Nitrogen (PON), Particulate Organic Carbon (POC), Total Phosphorus (TP), and Ammonia (A).

Previous studies have demonstrated that Chl-a concentrations are strongly associated with Particulate Organic Matter. In addition, total phosphorus and ammonia are key indicators of eutrophication and crucial nutrient sources for algae proliferation, as reported by several studies highlighting their significance in HAB occurrence (Havens, 2003; Zhai et al., 2009; Zhang et al., 2024; Dai et al., 2012; Wurtsbaugh et al., 2019). Similarly, our results suggested that increases in total phosphorous and ammonia correspondingly lead to increases in Chl-a concentration.

Table 6. SHAP values of the 5 most important features in the HAB prediction for ML models

ML Model	Input Features (mean |SHAP|)				
Lasso	TP (25)	Turb (6.5)	A (2.0)	TDP (1.5)	POC (0.5)
Ridge	TP (35)	Turb (10)	A (2.5)	TDP (2.0)	POC (0.7)
KNN	N (6.0)	TDP (3.5)	DO (2.5)	Temp (2.0)	Cond (1.1)
DT	PON (20.0)	POC (6.0)	A (4.0)	Turb (2.5)	DO (2.0)
MLP	TP (15.0)	Turb (12.2)	A (10.0)	POC (5.3)	PON (2.0)
AdaBoost	PON (14.5)	POC (2.2)	A (1.8)	Temp (0.3)	N (0.1)
LightGBM	PON (17.7)	POC (7.5)	A (2.8)	Turb (2.7)	TP (2.5)
RF	PON (9.5)	POC (6.0)	A (2.5)	Turb (1.8)	Temp (1.5)
SVM	PON (24)	POC (12)	TP (7.5)	TDP (6.0)	N (5.9)
GB	PON (25)	POC (6)	TP (5)	Turb (5)	A (4.5)
XGBoost	PON (18)	POC (7)	A (3)	Turb (2.7)	Temp (2.5)
DF	PON (14)	POC (5)	A (2)	Turb (1.5)	N (1)

SHAP provides the direction of contribution to the prediction results in addition to the magnitude. Figure 5 represents one example of a SHAP summary plot for the distribution of the SHAP values for SVM and XGB ML models, showing the relative effect of each input variable on model performance. In this figure, the input features were sorted by SHAP value so that a feature with greater effect on the model performance was shown at a higher position. The colored dots represented the SHAP value of each sample in the data, whereas the color hue represented the actual value of the observed data from high (red) to low (blue) values.

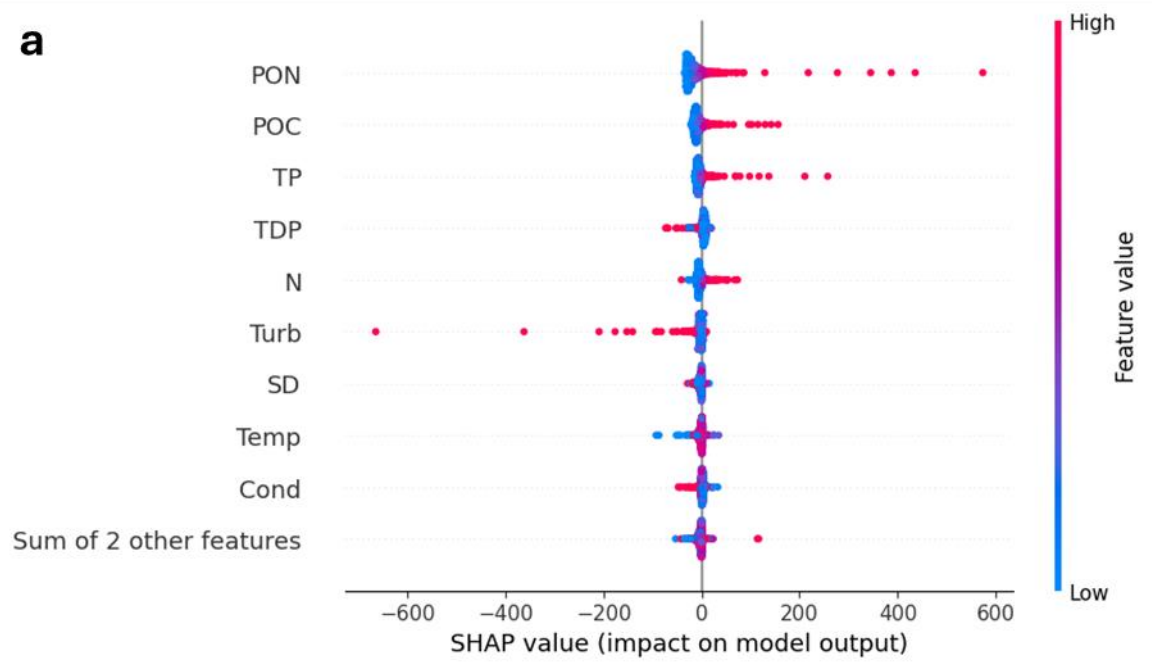

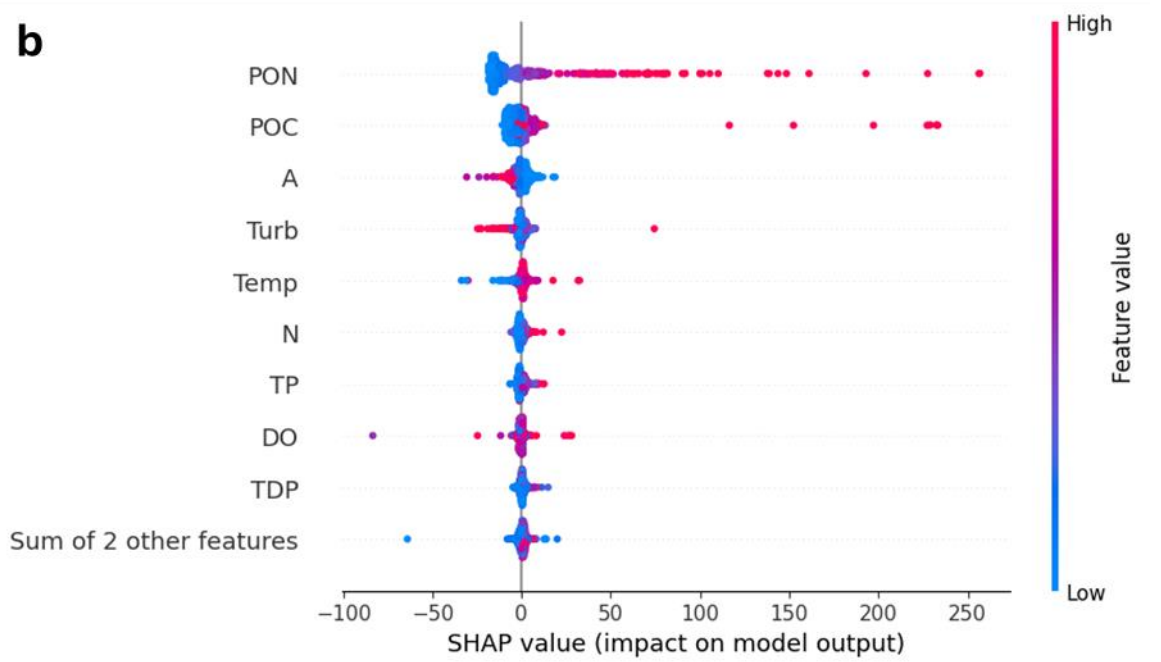

Figure 5. SHAP value of features and the impact on the model output for (a) SVM and (b) XGB models.

This figure provided an interpretable explanation of how the input features affected the model prediction. For both models (Figure 5), PON is located at the top of the figure, which suggests that PON had the greatest effect on performance. In addition, the SHAP value of PON increases as the feature value increases, indicating that PON contributes positively to algal bloom occurrence. This direction of the contribution of PON appeared commonly for all the ensemble-based ML models used in this study. This comprehensive feature-importance analysis guides us in understanding which factors are most influential in predicting HAB, aiding in model interpretation and refinement.

4. Conclusions

Predicting HABs is a major concern in devising a proper management strategy for governmental decision-making process. Thus, accurate prediction of HABs allows government to take proactive measures against these potential hazards. In recent years advanced ML algorithms have been increasingly used for HABs prediction, and it is necessary to improve the practical applicability of these models. In this study, we presented a comprehensive and comparative analysis of ensemble ML methods for predicting chlorophyll-a concentrations, representing a significant shift from traditional methods by developing a model capable of providing integrated predictions across multiple monitoring stations rather than focusing on single-location predictions or satellite imagery.

We have investigated the effectiveness of ensemble ML algorithms in predicting Chlorophyll-a (Chl-a) concentrations in the western basin of Lake Erie over an eight-year period (2013-2020). Then, we studied model fusion based on stacking and voting strategies aiming at improving the performance of weak ML algorithms. The high-performance ensemble ML models were then explained or interpreted using SHAP analysis. For the linear ML models, the most accurate model was the SVM with an R^2 value of 0.8160. The ensemble methods were

in general able to achieve higher accuracies than the linear ML models, with the highest performing being the XGB and DF with R^2 values of 0.8517 and 0.8544, respectively.

The fusion of weaker learners such as the KNN and DT with R^2 values of 0.6044 and 0.7190 respectively using the voting or stacking strategies could lead to a significant improvement of accuracy. However, the fusion of stronger learners would often not improve accuracy significantly, as demonstrated with the fusion of the MLP, KNN, SVM, and DT using the voting method. Our analysis revealed that several features significantly influenced the Chl-a concentrations in Lake Erie, identifying Particulate Organic Carbon (POC), Particulate Organic Nitrogen (PON), and Total Phosphorus (TP) as the most critical. We also found a correlation between increases in these factors and rising Chl-a concentrations, suggesting a potential link that warrants further investigation.

In summary, this study not only highlights the efficacy of the various ML models in HAB prediction but also contributes significantly to the field of environmental modeling by showing the potential of advanced ensemble machine learning techniques to enhance prediction accuracy and interpretability. The integration of explainable AI methodologies ensures that the model's predictions are transparent and actionable, facilitating better management strategies for mitigating the impacts of HABs. Moreover, we also determined the effect of the fusion of multiple weaker and stronger models on predictive accuracy for chlorophyll-a concentrations.

Although the overall prediction performance provided valuable insights, it is essential to recognize certain limitations in our study. The model was developed using only a limited number of stations due to missing data, and the training period was relatively short. Future research should focus on building larger datasets and broadening the scope of studies by continuously managing and preserving daily collected data.

Additionally, incorporating parameters such as meteorological data (e.g., air temperature, wind speed, precipitation, solar irradiance) and hydrodynamic data (e.g., water level, flow rate) could enhance the training process and improve prediction accuracy. Moreover, further refinement of the ensemble model's architecture and training process is necessary to boost its predictive capabilities. These advancements will be vital for enhancing environmental monitoring and management strategies, ultimately supporting the sustainability of aquatic ecosystems in the face of evolving environmental challenges.

5. References

Ahsan, M. M., Mahmud, M. P., Saha, P. K., Gupta, K. D., & Siddique, Z. (2021). Effect of data scaling methods on machine learning algorithms and model performance. Technologies, 9(3), 52.

Ai, H., Zhang, K., Sun, J., & Zhang, H. (2023). Short-term Lake Erie algal bloom prediction by classification and regression models. Water Research, 232, 119710.

Arashi, M., Roozbeh, M., Hamzah, N. A., & Gasparini, M. (2021). Ridge regression and its applications in genetic studies. Plos one, 16(4), e0245376.

Arrieta, A. B., Díaz-Rodríguez, N., Del Ser, J., Bennetot, A., Tabik, S., Barbado, A., ... & Herrera, F. (2020). Explainable Artificial Intelligence (XAI): Concepts, taxonomies, opportunities and challenges toward responsible AI. Information fusion, 58, 82-115.

Bauer, E., & Kohavi, R. (1999). An empirical comparison of voting classification algorithms: Bagging, boosting, and variants. Machine learning, 36, 105-139.

Bayar, S., Demir, I., & Engin, G. O. (2009). Modeling leaching behavior of solidified wastes using back-propagation neural networks. Ecotoxicology and environmental safety, 72(3), 843-850.

Baydaroğlu, Ö., Yeşilköy, S., Dave, A., Linderman, M., & Demir, I. (2024). Modeling of Harmful Algal Bloom Dynamics and Integrated Web Framework for Inland Waters in Iowa. EarthArxiv, 7075. https://doi.org/10.31223/X5S40X

Boegehold, A. G., Burtner, A. M., Camilleri, A. C., Carter, G., DenUyl, P., Fanslow, D., ... & Errera, R. (2023). Routine monitoring of western Lake Erie to track water quality changes associated with cyanobacterial harmful algal blooms. Earth System Science Data Discussions, 2023, 1-39.

Boyer, J. N., Kelble, C. R., Ortner, P. B., & Rudnick, D. T. (2009). Phytoplankton bloom status: Chlorophyll a biomass as an indicator of water quality condition in the southern estuaries of Florida, USA. Ecological indicators, 9(6), S56-S67.

Breiman, L. (2001). Random forests. Machine learning, 45, 5-32.

Buratti, F. M., Manganelli, M., Vichi, S., Stefanelli, M., Scardala, S., Testai, E., and Funari, E. (2017). Cyanotoxins: producing organisms, occurrence, toxicity, mechanism of action and human health toxicological risk evaluation, Arch. Toxicol., 91, 1049-1130.

Burkart, N., & Huber, M. F. (2021). A survey on the explainability of supervised machine learning. Journal of Artificial Intelligence Research, 70, 245-317.

Busari, I., Sahoo, D., Harmel, R. D., & Haggard, B. E. (2024). Prediction Of Chlorophyll-a As an Index of Harmful Algal Blooms Using Machine Learning Models. Journal of Natural Resources and Agricultural Ecosystems, 2(2), 53-61

Carmichael, W. W. and Boyer, G. L. (2016). Health impacts from cyanobacteria harmful algae blooms: Implications for the North American Great Lakes, Harmful Algae, 54, 194-212.

Carmichael, W. W., & Falconer, I. R. (1993). Diseases related to freshwater blue-green algal toxins, and control measures. In I.R. Falconer (Ed.). Algal toxins in seafood and drinking water (pp.187-209). London: Academic Press

Cha, Y., Shin, J., Go, B., Lee, D. S., Kim, Y., Kim, T., & Park, Y. S. (2021). An interpretable machine learning method for supporting ecosystem management: Application to species distribution models of freshwater macroinvertebrates. Journal of Environmental Management, 291, 112719.

Chen, T., & Guestrin, C. (2016, August). Xgboost: A scalable tree boosting system. In Proceedings of the 22nd acm sigkdd international conference on knowledge discovery and data mining (pp. 785-794).

Chen, X., Fu, Y., & Zhou, H. (2023). An approach of multi-element fusion method for harmful algal blooms prediction. Environmental Science and Pollution Research, 30(11), 32083-32094.

Dai, G. Z., Shang, J. L., & Qiu, B. S. (2012). Ammonia may play an important role in the succession of cyanobacterial blooms and the distribution of common algal species in shallow freshwater lakes. Global Change Biology, 18(5), 1571-1581.

Demir, I., Jiang, F., Walker, R. V., Parker, A. K., & Beck, M. B. (2009). Information systems and social legitimacy scientific visualization of water quality. In 2009 IEEE International Conference on Systems, Man and Cybernetics (pp. 1067-1072). IEEE.

Demiray, B. Z., Mermer, O., Baydaroğlu, Ö., & Demir, I. (2024). Predicting Harmful Algal Blooms Using Explainable Deep Learning Models: A Comparative Study. EarthArxiv, 7071. https://doi.org/10.31223/X58D9F

Derot, J., Yajima, H., & Jacquet, S. (2020). Advances in forecasting harmful algal blooms using machine learning models: A case study with Planktothrix rubescens in Lake Geneva. Harmful Algae, 99, 101906.

Friedman, J. H. (2001). Greedy function approximation: a gradient boosting machine. Annals of statistics, 1189-1232.

Ghatkar, J. G., Singh, R. K., & Shanmugam, P. (2019). Classification of algal bloom species from remote sensing data using an extreme gradient boosted decision tree model. International Journal of Remote Sensing, 40(24), 9412-9438.

Glibert, P. M. (2020). Harmful algae at the complex nexus of eutrophication and climate change. Harmful algae, 91, 101583.

Graham, J. L., Dubrovsky, N. M., & Eberts, S. M. (2016). Cyanobacterial harmful algal blooms and US Geological Survey science capabilities. US Department of the Interior, US Geological Survey.

Greene, S. B. D., LeFevre, G. H., & Markfort, C. D. (2021). Improving the spatial and temporal monitoring of cyanotoxins in Iowa lakes using a multiscale and multi-modal monitoring approach. Science of the Total Environment, 760, 143327.

Guo, G., Wang, H., Bell, D., Bi, Y., & Greer, K. (2003). KNN model-based approach in classification. In On the Move to Meaningful Internet Systems 2003: CoopIS, DOA, and ODBASE: OTM Confederated International Conferences, CoopIS, DOA, and ODBASE 2003, Catania, Sicily, Italy, November 3-7, 2003. Proceedings (pp. 986-996). Springer Berlin Heidelberg.

Hatwell, J., Gaber, M. M., & Atif Azad, R. M. (2020). Ada-WHIPS: explaining AdaBoost classification with applications in the health sciences. BMC Medical Informatics and Decision Making, 20, 1-25.

Havens, K. E. (2003). Phosphorus–algal bloom relationships in large lakes of south Florida: implications for establishing nutrient criteria. Lake and Reservoir Management, 19(3), 222-228.

Huang, J., Gao, J., & Zhang, Y. (2015). Combination of artificial neural network and clustering techniques for predicting phytoplankton biomass of Lake Poyang, China. Limnology, 16, 179-191.

Islam, S. S., Yeşilköy, S., Baydaroğlu, Ö., Yıldırım, E., & Demir, I. (2024). State-level multidimensional agricultural drought susceptibility and risk assessment for agriculturally prominent areas. International Journal of River Basin Management, 1-18.

Jeong, B., Chapeta, M. R., Kim, M., Kim, J., Shin, J., & Cha, Y. (2022). Machine learning-based prediction of harmful algal blooms in water supply reservoirs. Water Quality Research Journal, 57(4), 304-318.

Jiang, J., Zhou, H., Zhang, T., Yao, C., Du, D., Zhao, L., ... & Wu, X. E. (2022). Machine learning to predict dynamic changes of pathogenic Vibrio spp. abundance on microplastics in marine environment. Environmental Pollution, 305, 119257.

Jung, N. C., Popescu, I., Kelderman, P., Solomatine, D. P., & Price, R. K. (2010). Application of model trees and other machine learning techniques for algal growth prediction in Yongdam reservoir, Republic of Korea. Journal of Hydroinformatics, 12(3), 262-274.

Katin, A., Del Giudice, D., Hall, N. S., Paerl, H. W., & Obenour, D. R. (2021). Simulating algal dynamics within a Bayesian framework to evaluate controls on estuary productivity. Ecological Modelling, 447, 109497.

Ke, G., Meng, Q., Finley, T., Wang, T., Chen, W., Ma, W., ... & Liu, T. Y. (2017). Lightgbm: A highly efficient gradient boosting decision tree. Advances in neural information processing systems, 30.

Kim, Y. W., Kim, T., Shin, J., Lee, D. S., Park, Y. S., Kim, Y., & Cha, Y. (2022). Validity evaluation of a machine-learning model for chlorophyll a retrieval using Sentinel-2 from inland and coastal waters. Ecological Indicators, 137, 108737.

Kislik, C., Dronova, I., Grantham, T. E., & Kelly, M. (2022). Mapping algal bloom dynamics in small reservoirs using Sentinel-2 imagery in Google Earth Engine. Ecological Indicators, 140, 109041.

Kouakou, C. R., & Poder, T. G. (2019). Economic impact of harmful algal blooms on human health: a systematic review. Journal of water and health, 17(4), 499-516.

Liaw, A., & Wiener, M. (2002). Classification and regression by RandomForest. R news, 2(3), 18-22.

Lin, S., Liang, Z., Zhao, S., Dong, M., Guo, H., & Zheng, H. (2024). A comprehensive evaluation of ensemble machine learning in geotechnical stability analysis and explainability. International Journal of Mechanics and Materials in Design, 20(2), 331-352.

Liu, M., & Lu, J. (2014). Support vector machine—an alternative to artificial neuron network for water quality forecasting in an agricultural nonpoint source polluted river?. Environmental Science and Pollution Research, 21, 11036-11053.

Lombard, F., Boss, E., Waite, A. M., Vogt, M., Uitz, J., Stemmann, L., ... & Appeltans, W. (2019). Globally consistent quantitative observations of planktonic ecosystems. Frontiers in Marine Science, 6, 196

Lu, H., & Ma, X. (2020). Hybrid decision tree-based machine learning models for short-term water quality prediction. Chemosphere, 249, 126169.

Lundberg, S. M., & Lee, S. I. (2017). A unified approach to interpreting model predictions. Advances in neural information processing systems, 30.

Lundberg, S. M., Erion, G., Chen, H., DeGrave, A., Prutkin, J. M., Nair, B., ... & Lee, S. I. (2020). From local explanations to global understanding with explainable AI for trees. Nature machine intelligence, 2(1), 56-67.

Ly, Q. V., Tong, N. A., Lee, B. M., Nguyen, M. H., Trung, H. T., Le Nguyen, P., ... & Hur, J. (2023). Improving algal bloom detection using spectroscopic analysis and machine learning: A case study in a large artificial reservoir, South Korea. Science of The Total Environment, 901, 166467.

Magnuson, J. J., Webster, K. E., Assel, R. A., Bowser, C. J., Dillon, P. J., Eaton, J. G., ... & Quinn, F. H. (1997). Potential effects of climate changes on aquatic systems: Laurentian Great Lakes and Precambrian Shield Region. Hydrological processes, 11(8), 825-871.

Mellios, N. K., Moe, S. J., & Laspidou, C. (2020). Using Bayesian hierarchical modelling to capture cyanobacteria dynamics in Northern European lakes. Water Research, 186, 116356.

Mount, J., Sermet, Y., Jones, C.S., Schilling, K.E., Gassman, P.W., Weber, L.J., Krajewski, W.F. and Demir, I., (2024). An integrated cyberinfrastructure system for water quality resources in the Upper Mississippi River Basin. Journal of hydroinformatics, 26(8), pp.1970-1988.

Nourani, V., Khodkar, K., Baghanam, A. H., Kantoush, S. A., & Demir, I. (2023). Uncertainty quantification of deep learning–based statistical downscaling of climatic parameters. Journal of applied meteorology and climatology, 62(9), 1223-1242.

Paerl, H. W., Gardner, W. S., Havens, K. E., Joyner, A. R., McCarthy, M. J., Newell, S. E., ... & Scott, J. T. (2016). Mitigating cyanobacterial harmful algal blooms in aquatic ecosystems impacted by climate change and anthropogenic nutrients. Harmful Algae, 54, 213-222.

Paerl, H. W., & Paul, V. J. (2012). Climate change: links to global expansion of harmful cyanobacteria. Water research, 46(5), 1349-1363.

Paerl, H. W., Hall, N. S., & Calandrino, E. S. (2011). Controlling harmful cyanobacterial blooms in a world experiencing anthropogenic and climatic-induced change. Science of the total environment, 409(10), 1739-1745.

Park, Y., Cho, K. H., Park, J., Cha, S. M., & Kim, J. H. (2015). Development of early-warning protocol for predicting chlorophyll-a concentration using machine learning models in freshwater and estuarine reservoirs, Korea. Science of the Total Environment, 502, 31-41.

Park, J., Lee, W. H., Kim, K. T., Park, C. Y., Lee, S., & Heo, T. Y. (2022). Interpretation of ensemble learning to predict water quality using explainable artificial intelligence. Science of the Total Environment, 832, 155070.

Pereira, J. M., Basto, M., & Da Silva, A. F. (2016). The logistic lasso and ridge regression in predicting corporate failure. Procedia Economics and Finance, 39, 634-641.

Prabha, A., Yadav, J., Rani, A., & Singh, V. (2021). Design of intelligent diabetes mellitus detection system using hybrid feature selection based XGBoost classifier. Computers in Biology and Medicine, 136, 104664.

Ranstam, J., & Cook, J. A. (2018). LASSO regression. Journal of British Surgery, 105(10), 1348-1348.

Ratté-Fortin, C., Plante, J. F., Rousseau, A. N., & Chokmani, K. (2023). Parametric versus nonparametric machine learning modelling for conditional density estimation of natural events: Application to harmful algal blooms. Ecological Modelling, 482, 110415.

Rolim, S. B. A., Veettil, B. K., Vieiro, A. P., Kessler, A. B., & Gonzatti, C. (2023). Remote sensing for mapping algal blooms in freshwater lakes: A review. Environmental Science and Pollution Research, 30(8), 19602-19616.

Qiu, Y., Liu, H., Liu, F., Li, D., Liu, C., Liu, W., ... & Duan, H. (2023). Development of a collaborative framework for quantitative monitoring and accumulation prediction of harmful algal blooms in nearshore areas of lakes. Ecological Indicators, 156, 111154.

Quinlan, J. R. (1986). Induction of decision trees. Machine learning, 1, 81-106.

Sammartino, M., Buongiorno Nardelli, B., Marullo, S., & Santoleri, R. (2020). An artificial neural network to infer the Mediterranean 3D chlorophyll-a and temperature fields from remote sensing observations. Remote Sensing, 12(24), 4123.

Saeed, W., & Omlin, C. (2023). Explainable AI (XAI): A systematic meta-survey of current challenges and future opportunities. Knowledge-Based Systems, 263, 110273.

Sari, A. C. (2021). Lasso regression for daily rainfall modeling at Citeko Station, Bogor, Indonesia. Procedia Computer Science, 179, 383-390.

Shin, Y., Kim, T., Hong, S., Lee, S., Lee, E., Hong, S., ... & Heo, T. Y. (2020). Prediction of chlorophyll-a concentrations in the Nakdong River using machine learning methods. Water, 12(6), 1822.

Shin, J., Yoon, S., Kim, Y., Kim, T., Go, B., & Cha, Y. (2021). Effects of class imbalance on resampling and ensemble learning for improved prediction of cyanobacteria blooms. Ecological informatics, 61, 101202.

Sit, M., Seo, B. C., Demiray, B., & Demir, I. (2024). EfficientRainNet: Leveraging EfficientNetV2 for memory-efficient rainfall nowcasting. Environmental Modelling & Software, 106001.

Stubblefield, J., Hervert, M., Causey, J. L., Qualls, J. A., Dong, W., Cai, L., ... & Huang, X. (2020). Transfer learning with chest X-rays for ER patient classification. Scientific reports, 10(1), 20900.

Stumpf, R. P., Johnson, L. T., Wynne, T. T., & Baker, D. B. (2016). Forecasting annual cyanobacterial bloom biomass to inform management decisions in Lake Erie. Journal of Great Lakes Research, 42(6), 1174-1183.

Sutton, C. D. (2005). Classification and regression trees, bagging, and boosting. Handbook of statistics, 24, 303-329.

Tanir, T., Yildirim, E., Ferreira, C. M., & Demir, I. (2024). Social vulnerability and climate risk assessment for agricultural communities in the United States. Science of The Total Environment, 908, 168346.

Tewari, M., Kishtawal, C. M., Moriarty, V. W., Ray, P., Singh, T., Zhang, L., ... & Tewari, K. (2022). Improved seasonal prediction of harmful algal blooms in Lake Erie using large-scale climate indices. Communications Earth & Environment, 3(1), 195.

Wang, Y., Xie, Z., Lou, I., Ung, W. K., & Mok, K. M. (2017). Algal bloom prediction by support vector machine and relevance vector machine with genetic algorithm optimization in freshwater reservoirs. Engineering Computations, 34(2), 664-679.

Wang, Y., Chen, Z., Shao, H., & Wang, N. (2021, June). A KNN-based classification algorithm for growth stages of haematococcus pluvialis. In 2021 IEEE 4th Advanced Information Management, Communicates, Electronic and Automation Control Conference (IMCEC) (Vol. 4, pp. 6-9). IEEE.

Weber, L.J., Muste, M., Bradley, A.A., Amado, A.A., Demir, I., Drake, C.W., Krajewski, W.F., Loeser, T.J., Politano, M.S., Shea, B.R. and Thomas, N.W., (2018). The Iowa Watersheds Project: Iowa's prototype for engaging communities and professionals in watershed hazard mitigation. International journal of river basin management, 16(3), pp.315-328.

Weirich, C. A., & Miller, T. R. (2014). Freshwater harmful algal blooms: toxins and children's health. Current problems in pediatric and adolescent health care, 44(1), 2-24.

Wells, M. L., Trainer, V. L., Smayda, T. J., Karlson, B. S., Trick, C. G., Kudela, R. M., ... & Cochlan, W. P. (2015). Harmful algal blooms and climate change: Learning from the past and present to forecast the future. Harmful algae, 49, 68-93.

Wolpert, D. H. (1992). Stacked generalization. Neural networks, 5(2), 241-259.

Wu, N., Huang, J., Schmalz, B., & Fohrer, N. (2014). Modeling daily chlorophyll a dynamics in a German lowland river using artificial neural networks and multiple linear regression approaches. Limnology, 15, 47-56.

Wurtsbaugh, W. A., Paerl, H. W., & Dodds, W. K. (2019). Nutrients, eutrophication and harmful algal blooms along the freshwater to marine continuum. Wiley Interdisciplinary Reviews: Water, 6(5), e1373.

Xu, H., Windsor, M., Muste, M., & Demir, I. (2020). A web-based decision support system for collaborative mitigation of multiple water-related hazards using serious gaming. Journal of environmental management, 255, 109887.

Yan, Z., Kamanmalek, S., Alamdari, N., 2024. Predicting coastal harmful algal blooms using integrated data-driven analysis of environmental factors. Science of The Total Environment 912, 169253. https://doi.org/10.1016/j.scitotenv.2023.169253

Yeşilköy, S., & Demir, I. (2024). Crop yield prediction based on reanalysis and crop phenology data in the agroclimatic zones. Theoretical and Applied Climatology, 1-14.

Yildirim, E., & Demir, I. (2022). Agricultural flood vulnerability assessment and risk quantification in Iowa. Science of The Total Environment, 826, 154165.

Yu, H., & Kim, S. (2012). SVM Tutorial-Classification, Regression and Ranking. Handbook of Natural Computing, 1, 479-506.

Zhai, S., Yang, L., & Hu, W. (2009). Observations of atmospheric nitrogen and phosphorus deposition during the period of algal bloom formation in Northern Lake Taihu, China. Environmental management, 44, 542-551.

Zhang, D., Qian, L., Mao, B., Huang, C., Huang, B., & Si, Y. (2018). A data-driven design for fault detection of wind turbines using random forests and XGboost. IEEE Access, 6, 21020-21031.

Zhang, X., Li, Y., Zhao, J., Wang, Y., Liu, H., & Liu, Q. (2024). Temporal dynamics of the Chlorophyll a-Total phosphorus relationship and algal production efficiency: Drivers and management implications. Ecological Indicators, 158, 111339.

Zhou, Z. X., Yu, R. C., & Zhou, M. J. (2022). Evolution of harmful algal blooms in the East China Sea under eutrophication and warming scenarios. Water Research, 221, 118807.

Zhou, Z. H., & Feng, J. (2019). Deep forest. National science review, 6(1), 74-86.